



---

## Figures and figure supplements

Nanoconnectomic upper bound on the variability of synaptic plasticity

**Thomas M Bartol et al**

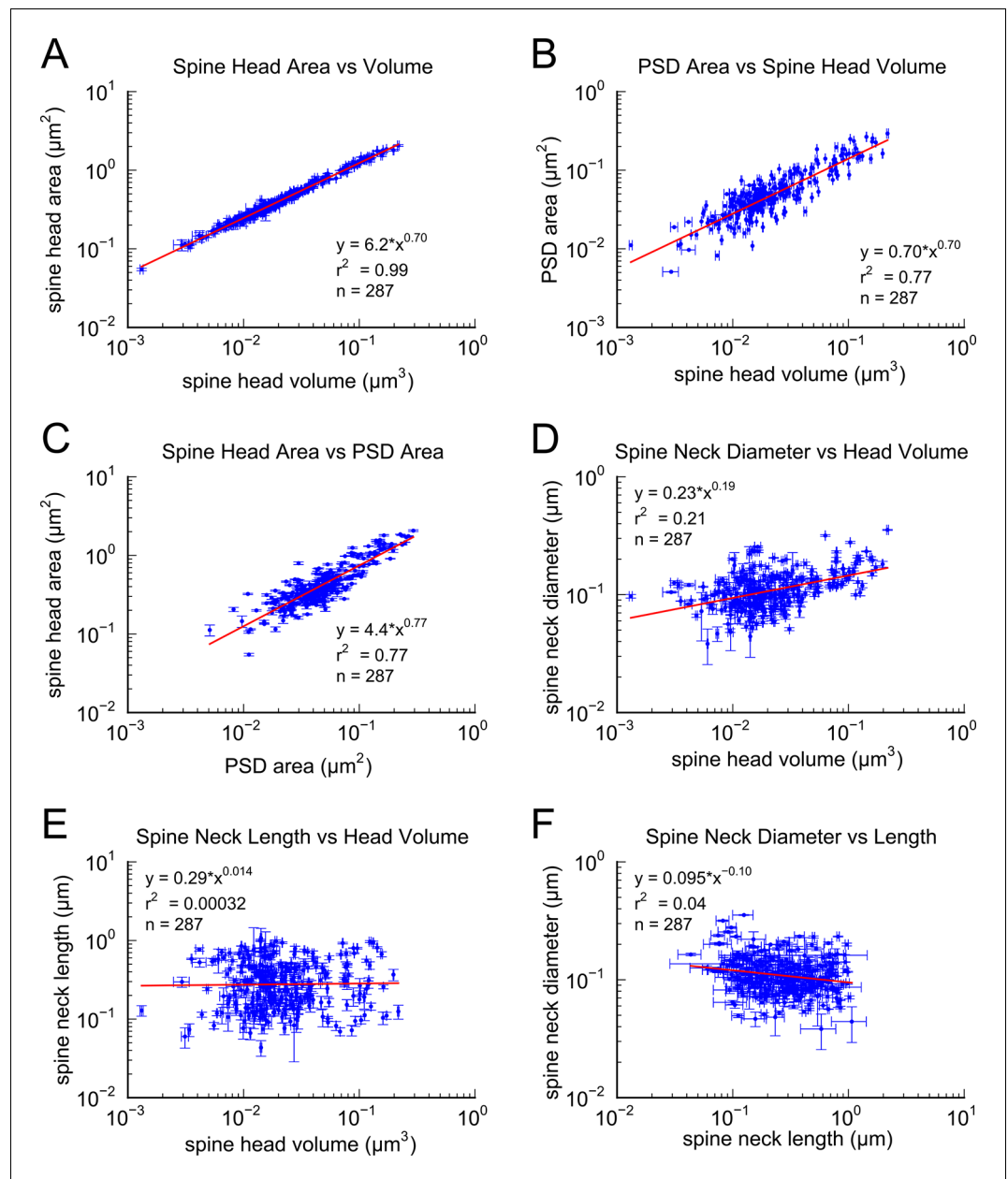


**Figure 1.** Spine head areas and PSD areas are correlated with spine head volumes, but neck length and neck diameter are not. Strong correlations between (A) Spine head area and spine head volume, (B) PSD area and spine head volume, and (C) Spine head area and PSD area. (D) Weak correlation between spine neck diameter and spine head volume. No correlation between (E) spine neck length and spine head volume and (F) spine neck diameter and spine neck length. Regression lines in red and error bars for each data point represent SEM based on multiple tracers who also edited each spine. Equations are based on the log-log distributions, with  $r^2$  values indicated, and  $n=287$  complete spines.

DOI: <http://dx.doi.org/10.7554/eLife.10778.003>

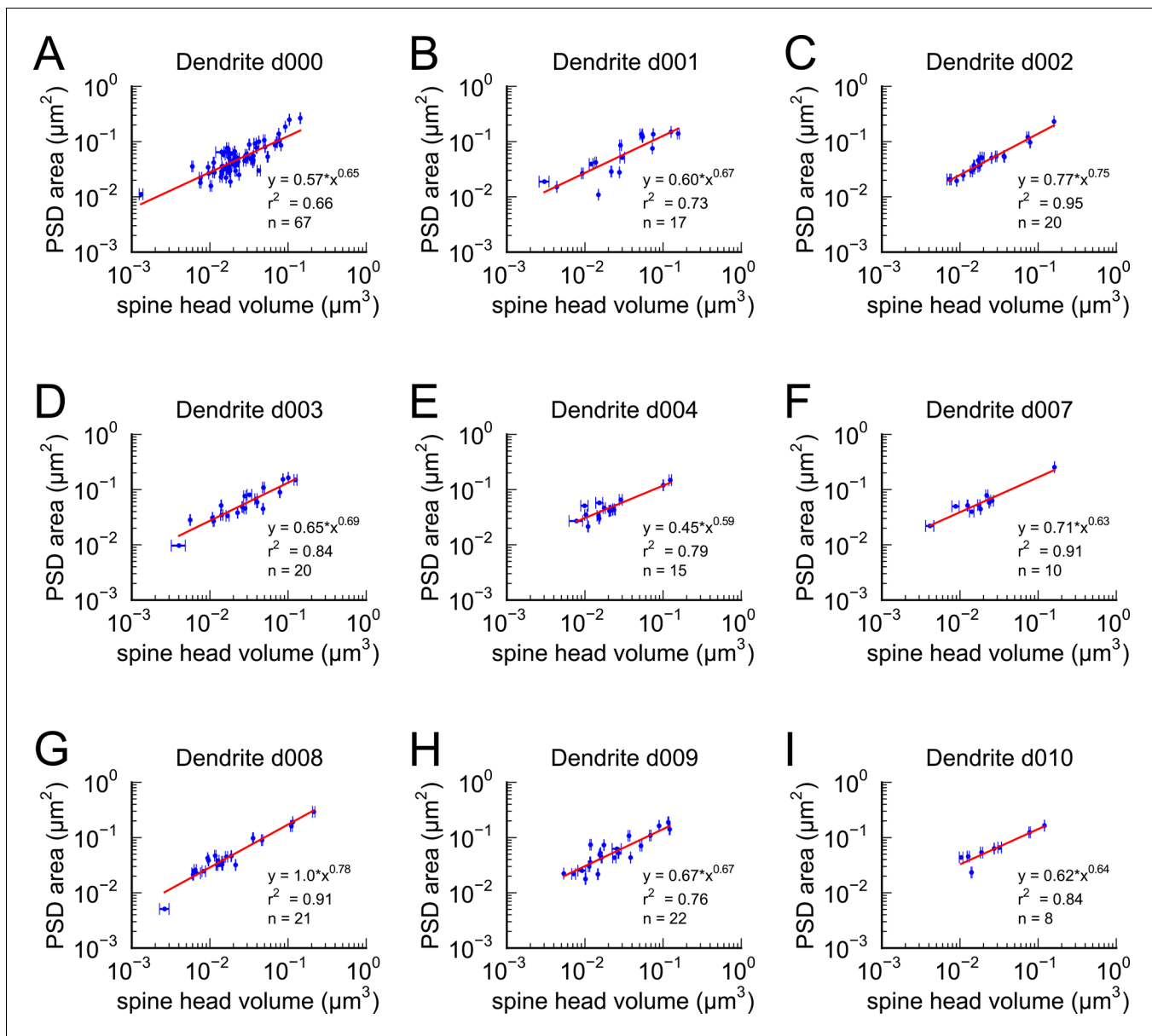


**Figure 1—figure supplement 1.** Area of postsynaptic density plotted against spine head volume. Nine individual dendrites all have similar slopes that are not significantly different showing the uniformity of this comparison across dendrites.

DOI: <http://dx.doi.org/10.7554/eLife.10778.004>

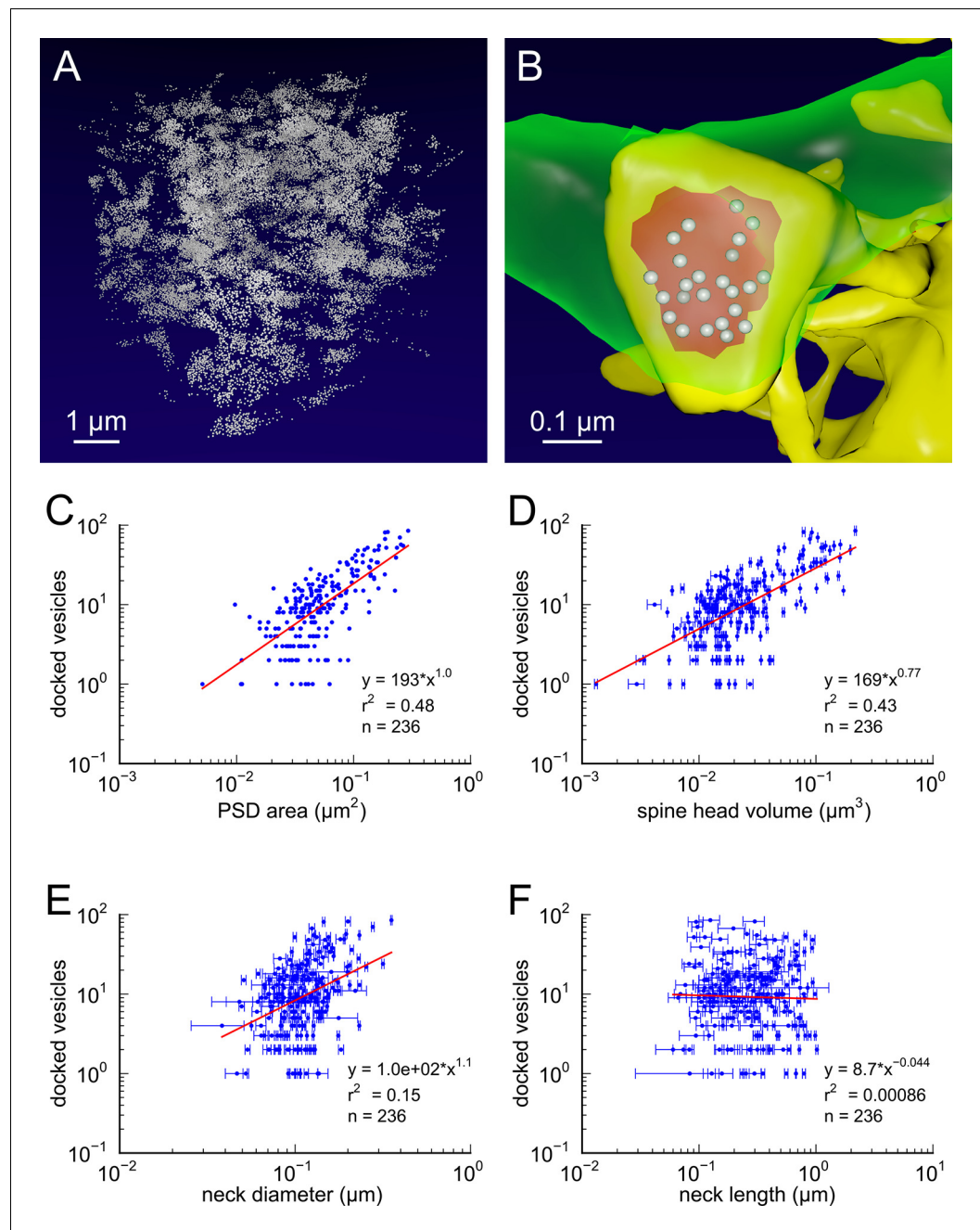


**Figure 2.** Presynaptic docked vesicle numbers are correlated with PSD areas, spine head volumes, and neck diameter, but not with neck length. (A) All 31,377 presynaptic vesicles. (B) En face view of the 24 docked vesicles (gray spheres) viewed through an axon (green) onto the PSD (red) of example spine (yellow). (C) Number of docked vesicles is correlated strongly with both PSD area and (D) spine head volume, weakly with (E) neck diameter, but is not correlated with (F) spine neck length. Regression lines, SEM (from multiple tracers), and  $r^2$  are as in Figure 1  $n = 236$  complete axonal boutons, each associated with one of the 287 complete spines. One human tracer marked PSDs and vesicles, hence no SEM for these two metrics.

DOI: <http://dx.doi.org/10.7554/eLife.10778.005>

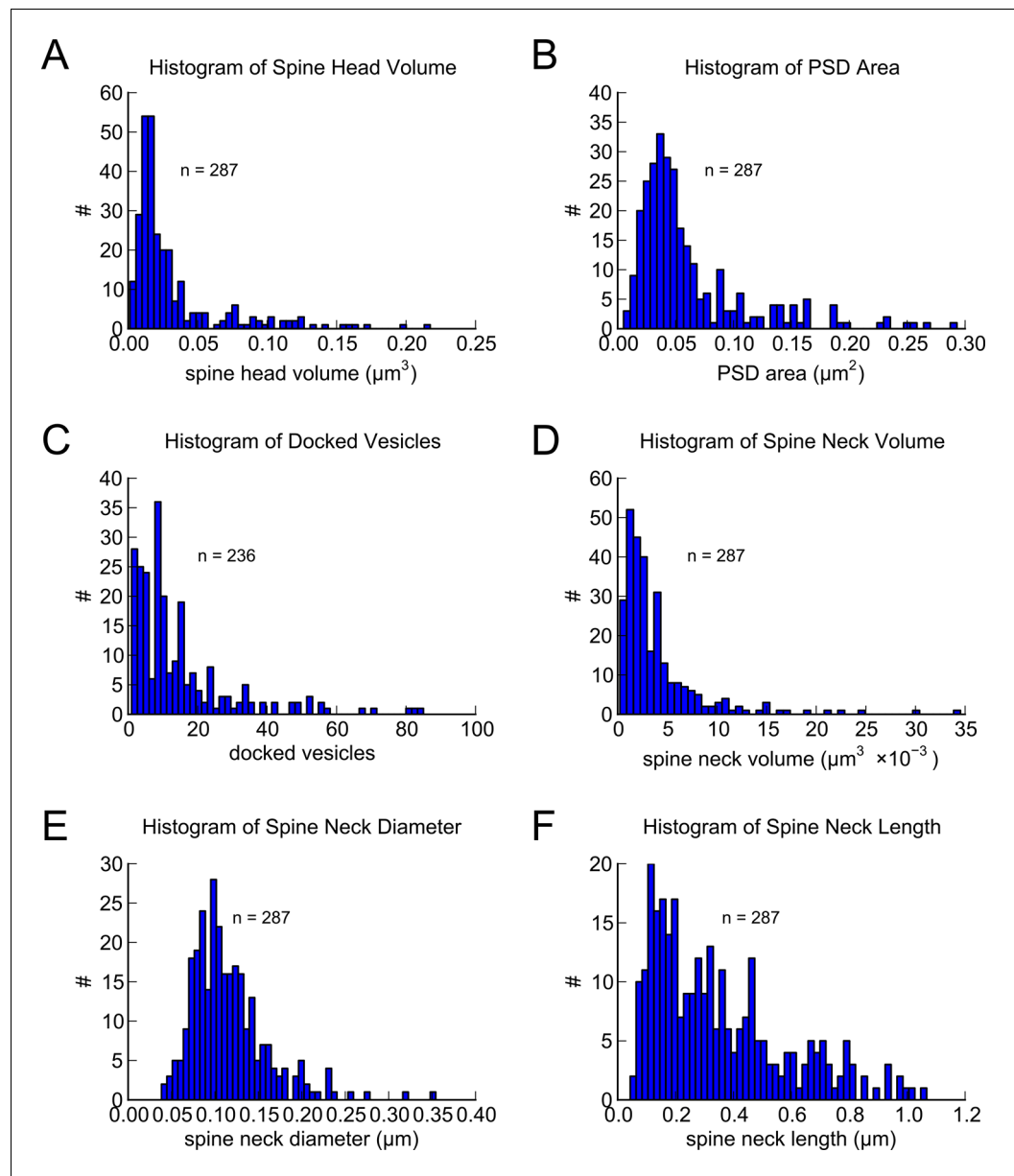


**Figure 3.** Morphometric analysis of 287 complete spines in reconstruction. Distributions of (A) spine head volumes, (B) PSD areas, (C) docked vesicles, (D) spine neck volumes, (E) spine neck diameters, and (F) spine neck lengths are highly skewed with a long tail.

DOI: <http://dx.doi.org/10.7554/eLife.10778.006>

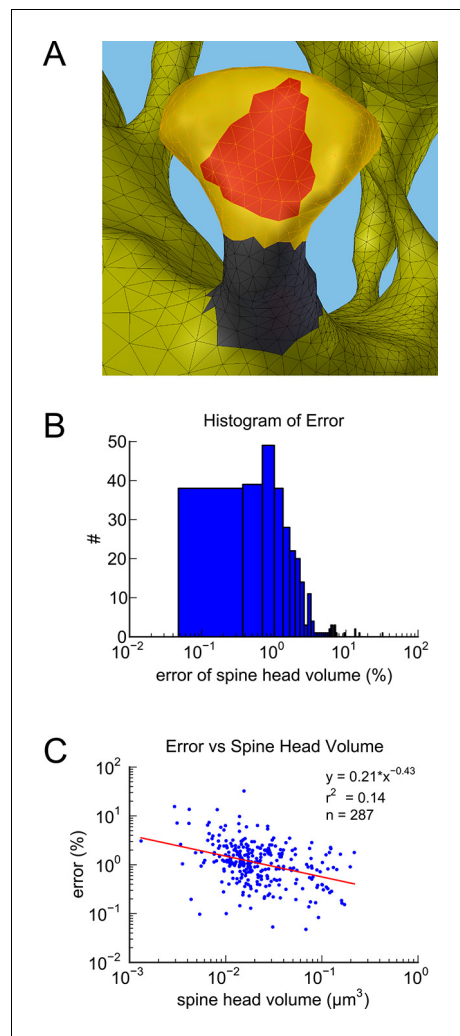


**Figure 3—figure supplement 1.** Spine measurement and estimation of measurement error. (A) Example segmentation of spine head (yellow), neck (gray), and PSD area (red). (B) Histogram of the measurement error across all spines measured. (C) Measurement error plotted against spine head volume.

DOI: <http://dx.doi.org/10.7554/eLife.10778.007>

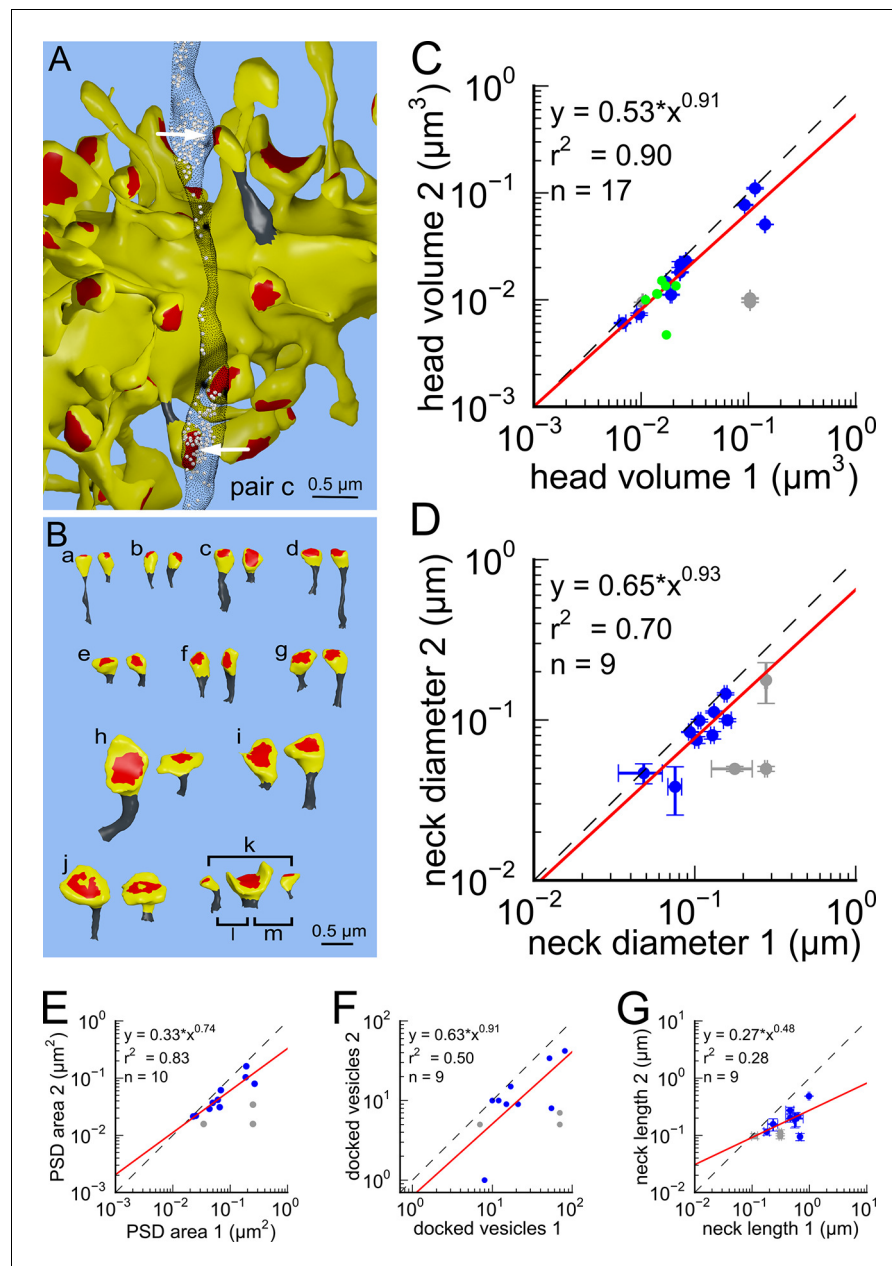


**Figure 4.** Spine head volumes, PSD areas and neck diameters, but not neck lengths, are highly correlated between pairs of axon-coupled same-dendrite spines. **(A)** Visualization of a pair of spines (gray necks) from the same dendrite (yellow) with synapses (red, indicated by white arrows) on the same axon (black stippling) with presynaptic vesicles (white spheres). **(B)** All axon-coupled same-dendrite spine pairs (colors as in A, pair c is elaborated in A). Strong correlations with slopes near 1 (dashed diagonal line) occur between paired **(C)** spine head volumes (slope = 0.91), **(D)** neck diameters (slope = 0.93), **(E)** PSD areas (slope = 0.74), and **(F)** docked vesicles (slope = 0.91); but not **(G)** spine neck lengths (slope = 0.48). Larger values from each pairing are plotted on the X axis. Regression lines (red) include the 10 a-j pairings (blue points) and 7 pairs from 2 additional animals (green points in (C)), but do not include triplet bouton pairings (k-m, gray points).

DOI: <http://dx.doi.org/10.7554/eLife.10778.008>

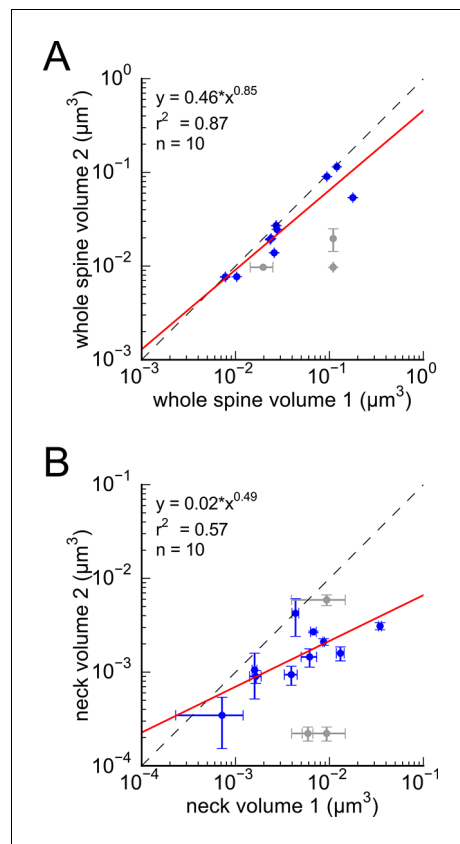


**Figure 4—figure supplement 1.** Analysis of whole spine volume and spine neck volume of axon-coupled same dendrite spines. **(A)** Whole spine volumes of pairs of axon-coupled spines on the same dendrite are highly correlated and significantly different from random pairs (KS test  $p = 0.018$ ). **(B)** Correlation of neck volumes of pairs of axon-coupled spines on the same dendrite are not significantly different from random pairs (KS test  $p = 0.74$ ). Larger value in each pair is plotted on the X axis. Regression lines shown in red. Equations are based on regression of log-log distributions, with  $r^2$  values indicated.

DOI: <http://dx.doi.org/10.7554/eLife.10778.009>



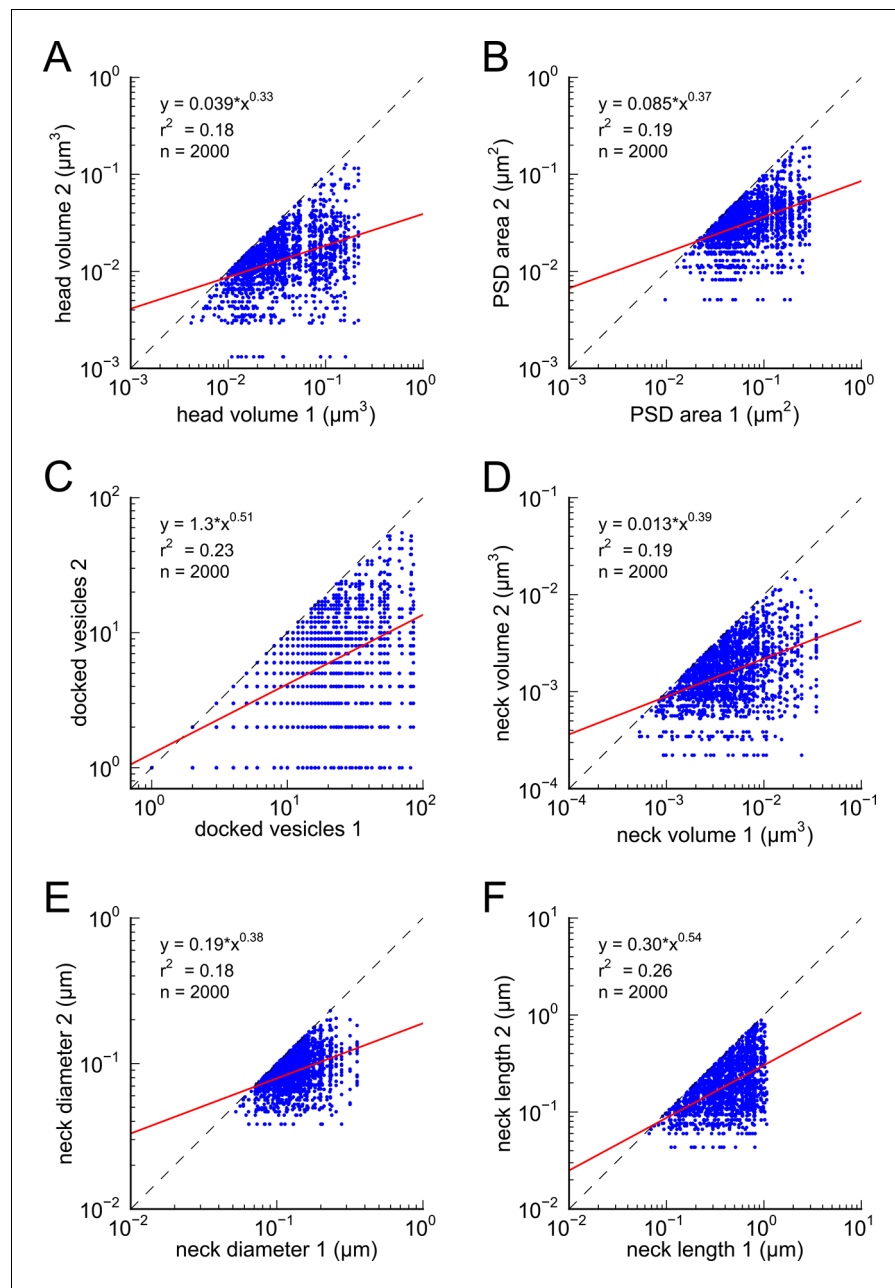


**Figure 4—figure supplement 2.** Analysis of spines paired randomly. Distributions represent random pairings of (A) spine head volumes, (B) PSD areas, (C) docked vesicles, (D) neck volumes, (E) neck diameters, and (F) neck lengths, from the population of complete spines in the reconstruction. Larger value in each pair is plotted on the X axis. Regression lines shown in red. Error bars for each data point are not shown for clarity. Equations are based on regression of log-log distributions, with  $r^2$  values indicated.

DOI: <http://dx.doi.org/10.7554/eLife.10778.010>

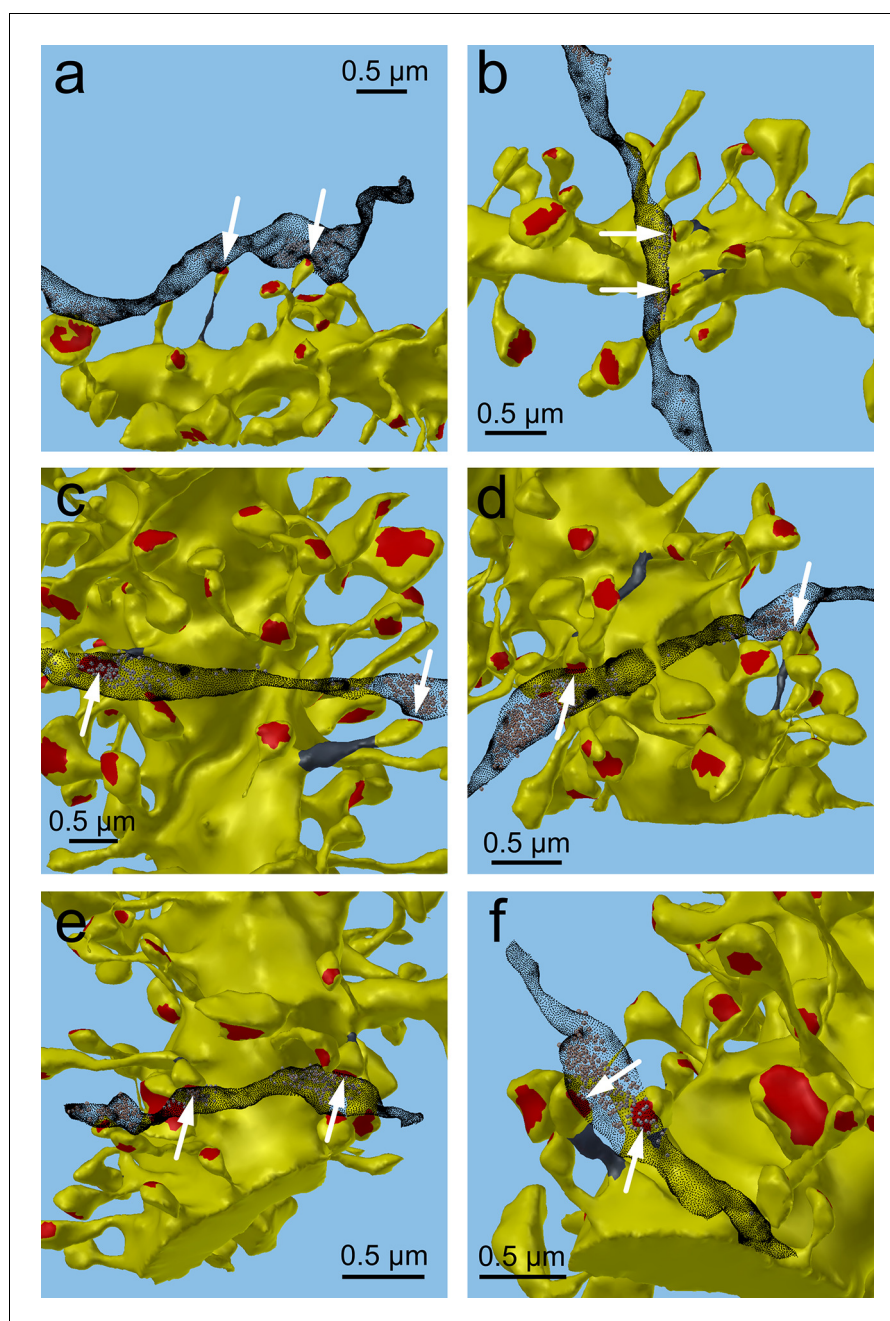


**Figure 4—figure supplement 3.** Axon-coupled same dendrite pairs a–f. Large white arrows indicate the red PSDs of the spine pairs, the edited necks are dark gray, and the axons are stippled black with vesicles inside. These illustrate how the axon weaves through the neuropil, synapses with two spines yet passes by others.

DOI: <http://dx.doi.org/10.7554/eLife.10778.011>

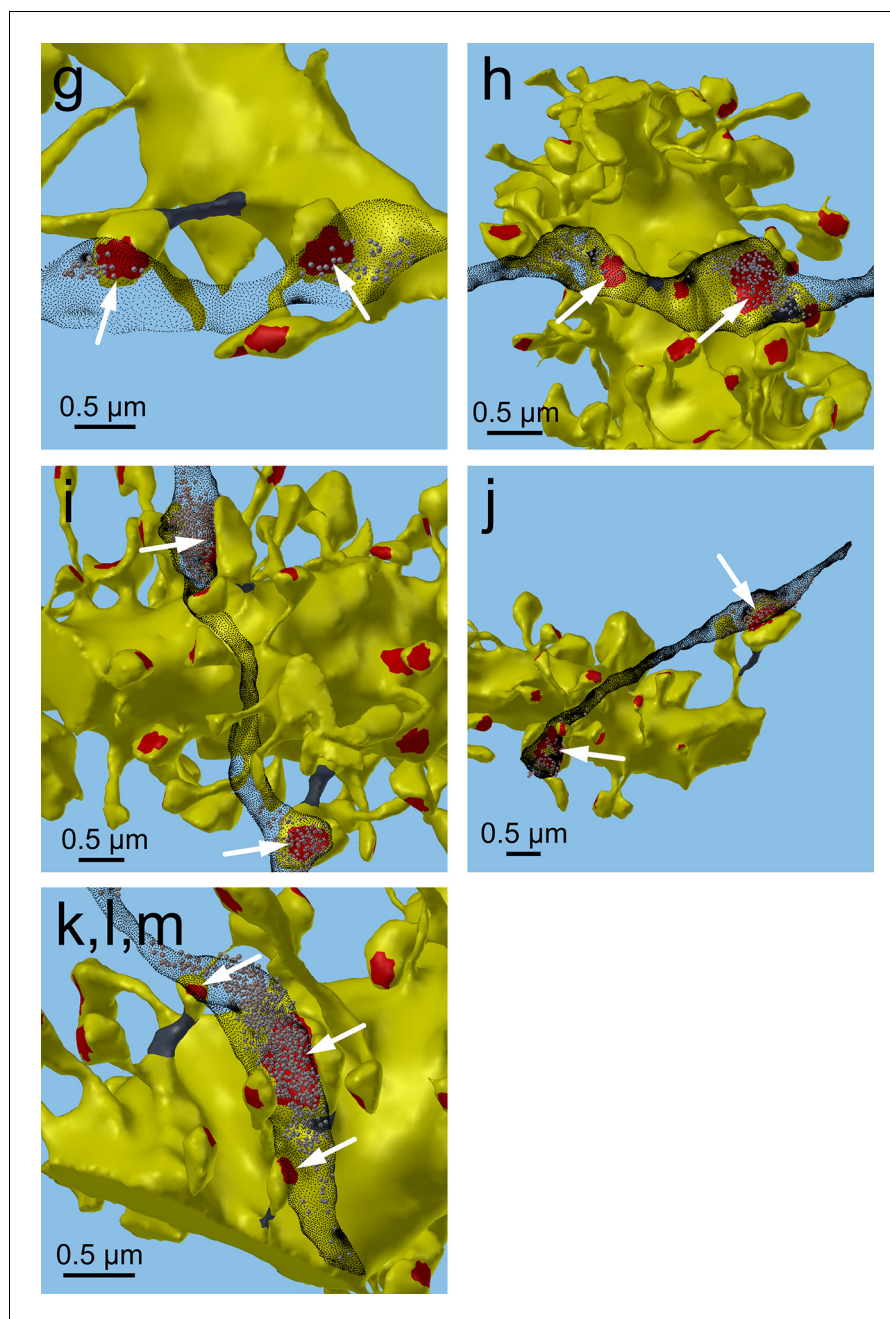


**Figure 4—figure supplement 4.** Axon-coupled same-dendrite pairs g-m, illustrated in same way as in **Figure 4—figure supplement 3**.

DOI: <http://dx.doi.org/10.7554/eLife.10778.012>

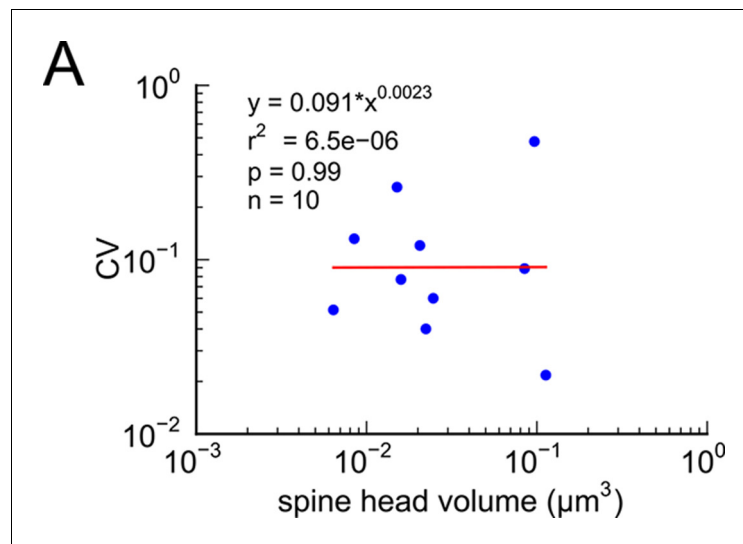


**Figure 5.** CV of axon-coupled spines on the same dendrite does not vary with spine size. There is no significant correlation, which implies that paired small synapses are as precisely matched as paired large synapses.

DOI: <http://dx.doi.org/10.7554/eLife.10778.013>

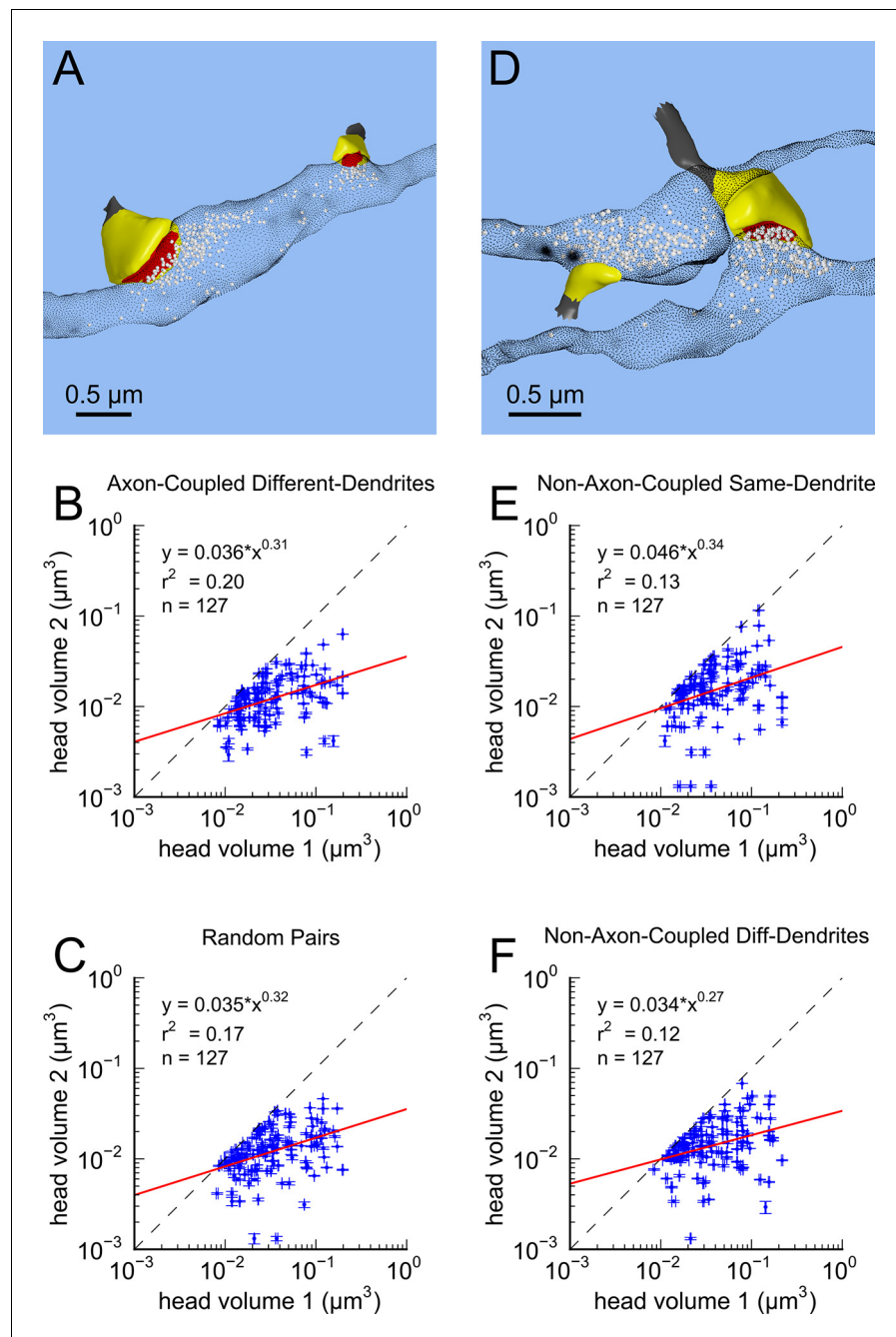


**Figure 6.** Paired spine head volumes are not correlated when they are not both axon and dendrite coupled. (A) Representative visualization and (B) plot showing lack of correlation between spine head volumes of all pairs of axon-coupled spines on different dendrites ( $n=127$ ). (C) Similarly, randomly associated pairs of spine head volumes were not correlated. (D) Representative visualization and plots show lack of correlation between spine head volumes from randomly selected pairs ( $n=127$ ) of non-axon-coupled spines (E) on the same or (F) different dendrites. Color scheme and regression analyses as in **Figure 4**.

DOI: <http://dx.doi.org/10.7554/eLife.10778.014>

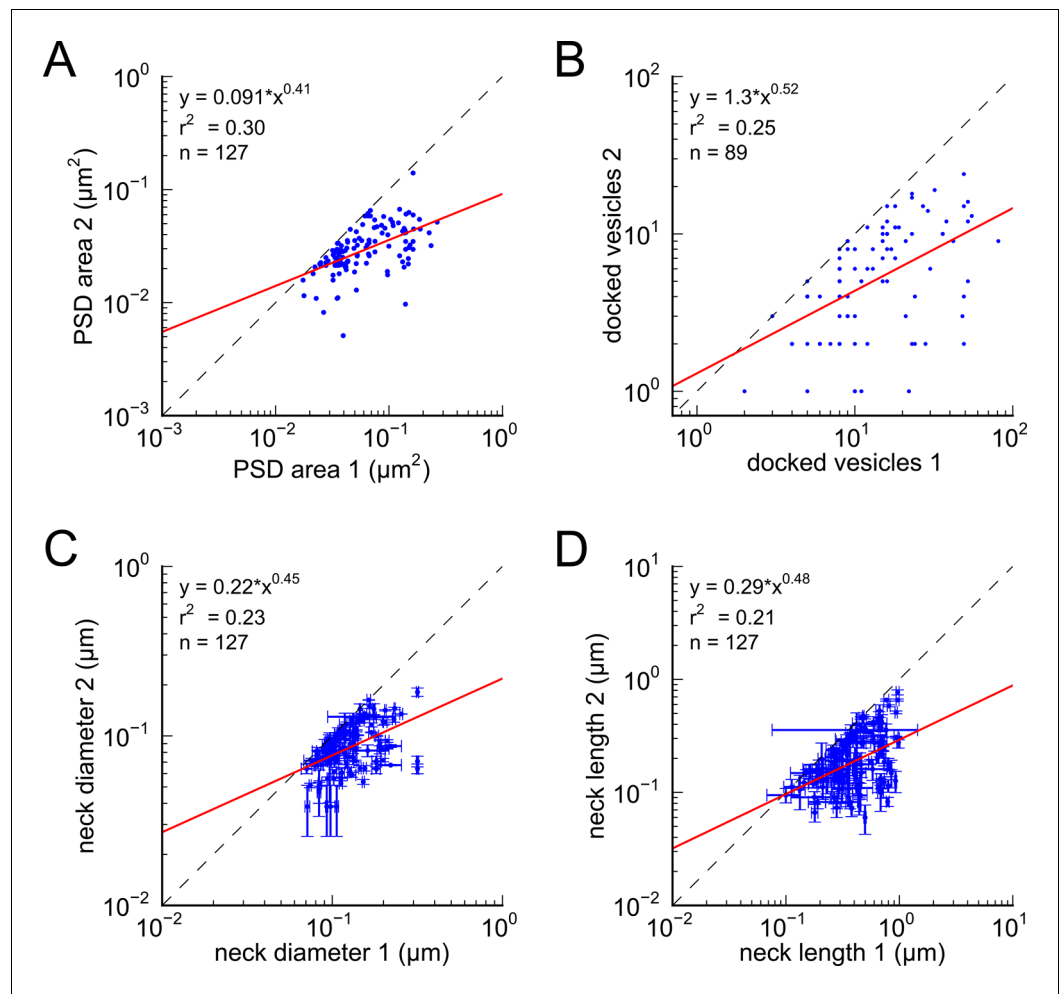


**Figure 6—figure supplement 1.** Morphologies of PSD, docked vesicles, and necks are not correlated when spines are not both axon and dendrite coupled. There is no correlation between (A) PSD areas, (B) docked vesicles, (C) neck diameters, and (D) neck lengths, in pairs of axon-coupled spines on different dendrites.

DOI: <http://dx.doi.org/10.7554/eLife.10778.015>



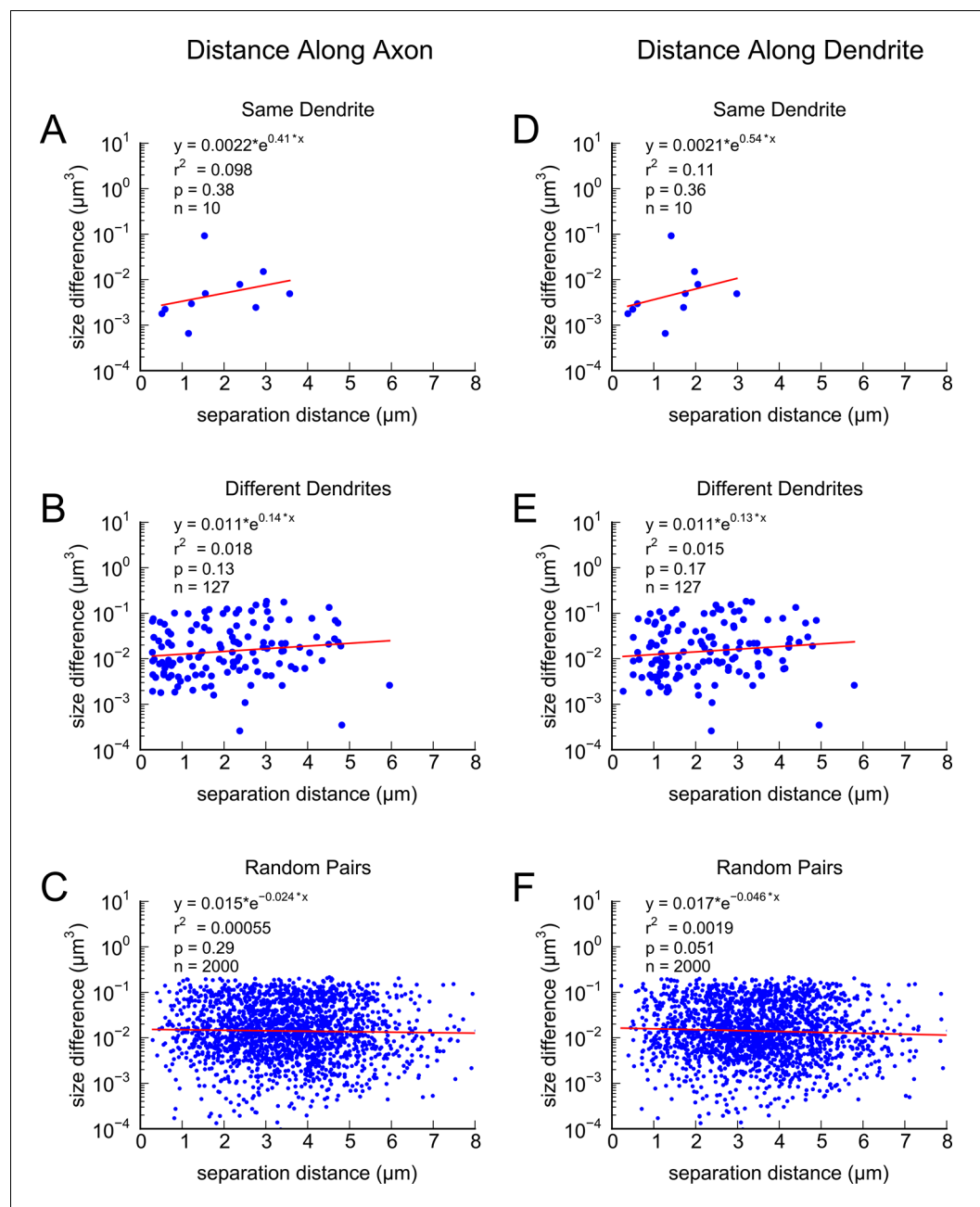


**Figure 6—figure supplement 2.** Difference in volume between pairs of axon-coupled spines exhibit a weak trend with separation distance. Differences in spine head volumes plotted against: **A)** Distance along the axon for axon-coupled spines on the same dendrite; **B)** Distance along the axon for axon-coupled spines on different dendrites; **C)** Distance along the axon for randomly paired spines; **D)** Distance along the dendrite for axon-coupled spines on the same dendrite; **E)** Distance along the dendrite for axon-coupled spines on different dendrites; **F)** Distance along the dendrite for randomly paired spines.

DOI: <http://dx.doi.org/10.7554/eLife.10778.016>

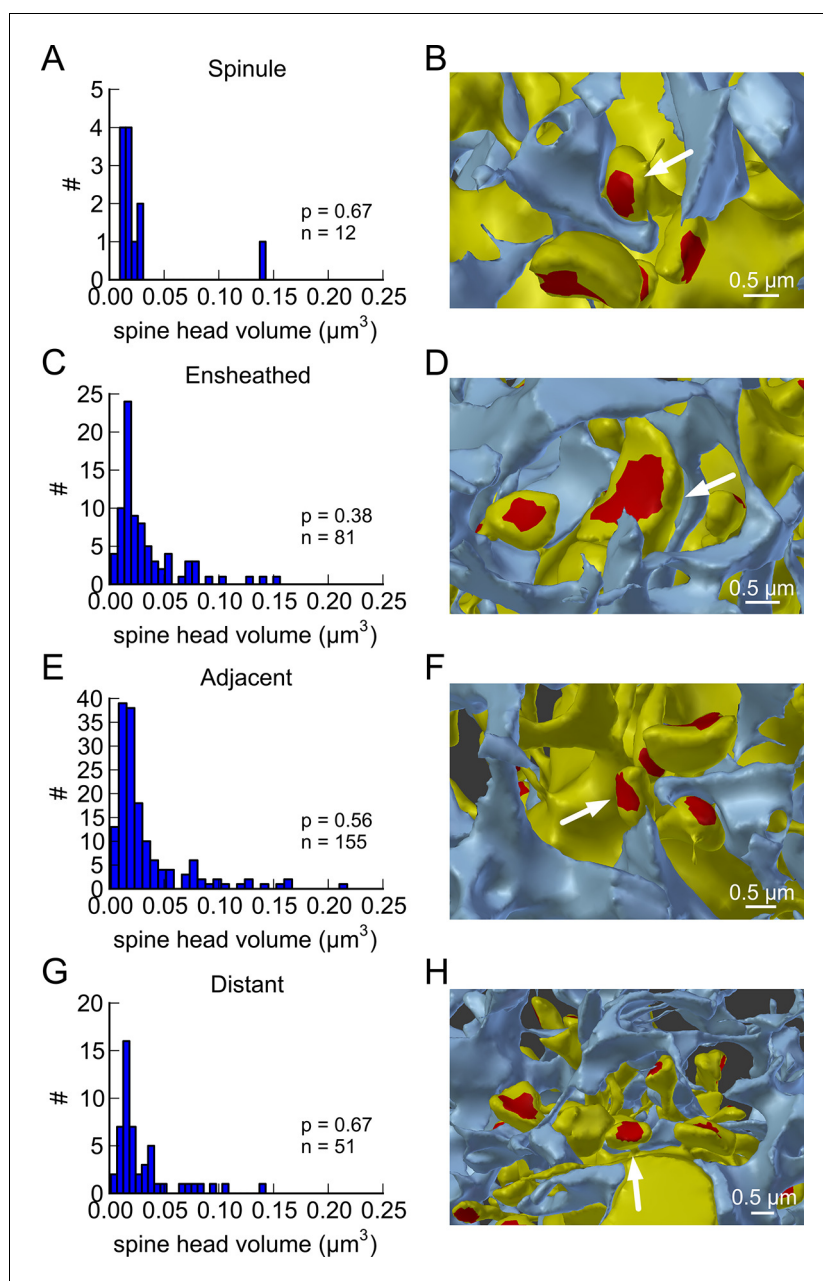


**Figure 7.** Proximity of the glial cell to axon-coupled dendritic spines on either the same or different dendrites. Proximity of astrocytic glial processes is not significantly correlated with spine head volumes of axon coupled pairs. (A) Histogram of spine head volume for spines that contain a spinule that is engulfed within the glial process ('spinule'). (B) Representation of an engulfed spinule. (C) Histogram of spine head volume for spines that are surrounded by and making contact with a glial process ('ensheathed'). (D) Representation of 'ensheathed' spine. (E) Histogram of spine head volume for spines that are proximal but not contacting a glial process ('adjacent'). (F) Representation of 'adjacent' spine. (G) Histogram of spine head volume for spines that are distant from any glial process. (H) Representation of a spine 'distant' from the glial process. The KS p value is shown on each inset and indicates that none of these distributions differ from the distribution for the whole population of spines.

DOI: <http://dx.doi.org/10.7554/eLife.10778.017>



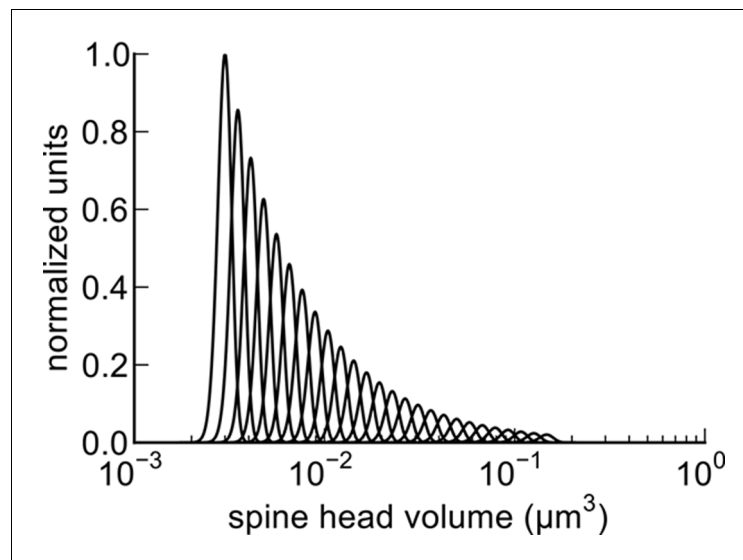


**Figure 8.** Distinguishable spine sizes. Over the factor of 60 range in spine head volumes from the data set there are 26 distinguishable intervals of spine sizes with a discrimination probability of 69% for each interval based on signal detection theory (Green and Swets, 1966; Schultz, 2007). The graph illustrates how distinct Gaussian distributions of spine sizes, each with a certain mean size and standard deviation, covers the entire range of spine head sizes on a log scale. The CV of each distribution is a constant value of 0.083 (Figure 5) and the intervals are spaced to achieve a total of 31% overlap with adjacent intervals giving a 69% discrimination threshold (see Materials and Methods). Note that the constant CV observed in the data set (Figure 5) means that the intervals appear uniform in width and spacing on a logarithmic scale. This is a form of non-uniform quantization which efficiently encodes the dynamic range of synaptic strengths at constant precision.

DOI: <http://dx.doi.org/10.7554/eLife.10778.018>